

**Production of Cyclohexylene-Containing Diamines in Pursuit of Novel
Radiation Shielding Materials**

Norah Gerow Bate

Asheville, North Carolina

Bachelor of Science, College of William & Mary, 2009

A Thesis presented to the Graduate Faculty
of the College of William and Mary in Candidacy for the Degree of
Master of Science

Department of Chemistry

The College of William and Mary
May, 2011

APPROVAL PAGE


This Thesis is submitted in partial fulfillment of
the requirements for the degree of

Master of Science

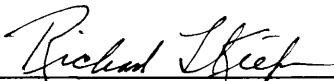


Nerah Gerow Bate

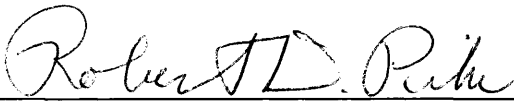
Approved by the Committee, March, 2011



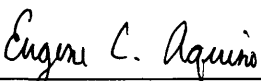
Committee Chair
Professor Emeritus Dr. Robert A. Orwoll, Chemistry
College of William & Mary



Professor Emeritus Dr. Richard L. Kiefer, Chemistry
College of William & Mary



Garrett-Robb-Guy Professor Dr. Robert D. Pike, Chemistry
College of William & Mary



Dr. Eugene C. Aquino
International Scientific Technologies, Inc.

ABSTRACT PAGE

Deep space radiation poses a formidable threat in space exploration. Current forms of radiation shielding materials are unequal to the task of protecting personnel and equipment from the detrimental impact of prolonged exposure to galactic cosmic radiation (GCR), neutrons, and high energy electromagnetic radiation. Before further expeditions can be undertaken, it is necessary to produce more effective shielding materials.

High performance polymers have the potential for excellent radiation shielding capabilities in the form of high hydrogen content. Hydrogen is an especially suitable element on a unit to mass basis due to its ability to slow high-energy GCR through Coulombic interactions. Additionally, high performance polymers have the advantages of high thermal and mechanical stability, lent by increased aromatic character. Additionally, these polymers are generally lightweight and are tailorable through alterations in monomer structure, allowing for the production of materials with desirable properties.

This research has concentrated on the production of novel cyclohexylene-containing diamine monomers which were synthesized in an effort to maximize hydrogen content without compromising the desirable mechanical or thermal properties of the polymers. Three novel diamines were produced along with their bisphenol and dinitro precursors. The crystal structures of the bisphenol and dinitro compounds were also ascertained. Additionally, low molecular weight polyimides were synthesized by combining each of the three diamines with benzophenone-3,3',4,4'-tetracarboxylic dianhydride (BTDA). These compounds provide an interesting route to the production of more effective shielding materials.

ACKNOWLEDGEMENTS

I would like to thank Dr. Robert Orwoll for all his help throughout my academic career and for putting up with my eccentricities for so long. Thank you to Dr. Elizabeth Harbron for the idea for the initial bisphenol synthesis, which got me off on the right foot. Thank you to Dr. Robert Pike for his extensive and invaluable assistance with the X-ray determinations of several of the synthesized compounds. Thank you to Dr. Robert Hinkle for his help in purification of the final diamine products. Thank you to Dr. Richard Kiefer and Dr. Eugene Aquino for their advice in my research. Thank you to Dr. Christopher Abelt for his patience with my questions. Finally thank you to Madeline Nestor, Brooklynd Saar, Jaeton Glover, Katie Peth, Ajara Rahman, and countless others for keeping me sane by fielding my rants. I could not have survived without you.

TABLE OF CONTENTS

Introduction	1
Barriers	1
• GCR	2
• Neutrons	3
• High-Energy Electromagnetic Radiation	4
Proposed Solution	5
Background Research	7
• Polyimides	7
◦ Properties	7
◦ Monomer Production	7
◦ Polymer Production	10
• Gadolinium Modification	12
Experimental Methods	13
• Materials	13
• Testing	13
• Monomer Synthesis	13
◦ Bisphenol	13
◦ Dinitro	16
◦ Diamine	20
• Diamine Purification	23
• Dianhydride Purification	23
• Polyimide Synthesis	23
◦ TED/BTDA	23
◦ TBD/BTDA	25
◦ TMD/BTDA	25
◦ TED/UDA	25
◦ TBD/UDA	26
• Gadolinium Salt Production	26
Results and Discussion	27
• Bisphenol Monomer	27
• Dinitro Production and Purification	28
• Diamine Production	32
• Polyimidization	34
• Gadolinium Addition	35
• Thermal Properties	36
Conclusion	41
Future Research	42
Funding	42
Appendix I	43
References	48

INDEX OF TABLES AND FIGURES

FIGURE NUMBER:

1) Bisphenol production from a ketone and a phenol	7
2) Mechanism for the reaction of a ketone (acetone) and a phenol	8
3) Synthesis of a dinitro compound from a bisphenol and 4-chloronitrobenzene	9
4) Diamine synthesis by hydrogenation of a dinitro compound	10
5) Polyimide synthesis using BTDA and TED monomers	11
6) Bisphenol precursors	14
7) Dinitro precursors	17
8) Diamine monomers	20
9) TED bisphenol crystal structure	27
10) TBD bisphenol crystal structure	28
11) TMD bisphenol crystal structure	28
12) TED dinitro crystal structure	30
13) TBD dinitro crystal structure	31
14) TMD dinitro crystal structure	31
15) Polyimides and their glass transition temperatures	38

TABLE NUMBER:

1) Polymer thermal properties and hydrogen content	36
2) Hydrogen content of selected polyimides	40

INTRODUCTION:

In the search for more complete knowledge of the galaxy around us, NASA has begun plans for a new wave of journeys further into our solar system with a view to manned landings on asteroids and the possibility of space habitats. These ventures provide an opportunity to broaden our awareness of the universe. Over the past several decades, the reach of scientific exploration has extended further and further outward, with surveying instruments on Mars and unmanned satellites monitoring Saturn. As the technology advances, privately owned companies are springing up to offer commercial flights. With this increased interest comes increased concern for the dangers inherent in space travel.

BARRIERS:

In preparation for increased space exploration, NASA has identified a need for new, more efficient radiation shielding materials. As a space vehicle travels further from Earth, it encounters increased radiation levels and more varied types of radiation. The surface of the earth is protected from many types of radiation by both the atmosphere and Earth's magnetic field. Traditional forms of shielding are ill-equipped to deal with radiation outside the magnetic field and have, in fact, been shown to worsen the effects through nuclear fragmentation.¹

The Earth's magnetic field extends outward into space trapping a variety of energetic, charged particles in two regions known as the Van Allen belts. The outer belt exists in a swath starting about three earth radii from the planet's surface and extends outward to ten earth radii above the surface. The inner belt begins about a hundredth of

an earth radius and extends out to about 1.5 earth radii above the surface. These belts contain charge particles from the sun and from sources outside the solar system. The earth's magnetic field deflects the incoming charged particles, causing them to travel in the belts around earth rather than reaching the earth's surface.

Galactic cosmic radiation (GCR) is largely deflected by the Van Allen belts while X-rays, gamma rays, and UV radiation are absorbed by the Earth's atmosphere. Without these protective layers, a spacecraft and its inhabitants are left vulnerable to these harmful radiations. Additionally, the occupants of any spacecraft which encounters these forms of radiation must also be concerned with the effects of free neutrons which are produced as secondary radiation from fragmentation caused by GCR interacting with the walls and contents of the spacecraft.

So long as expeditions are brief, damage caused by radiation is relatively inconsequential. However, a trip to Mars or an asteroid, or the establishment of a lunar habitat will require exposure of sufficiently long duration to cause detrimental effects to both equipment and personnel as a result of these radiations. This research aims to address the issues associated with galactic cosmic radiation, high-energy electromagnetic radiation, and neutrons.

1) GCR:

Galactic cosmic radiation is composed of bare nuclei of elements ranging in size from hydrogen up through iron. The radiation is largely composed of hydrogen (85%) and helium (14%).¹ A small but significant fraction of these nuclei travel at tremendous velocities, giving the particles large kinetic energies. When translated into a collision

with any structural, instrumental, or biological material, the large kinetic energy can mean a great deal of damage; the higher the atomic number of the incident nucleus, the greater the damage done during impact.

Those GCR nuclei with high atomic number are referred to as HZE particles and are of greatest concern in the quest for more effective shielding materials. Because of their high mass they have the capacity to completely penetrate traditional shielding materials. As the HZE pass through the shield, they interact with the atoms in the shielding material itself, producing higher levels of radiation through nuclear fragmentation. The fragmentation produces secondary forms of radiation such as additional nuclei, some of which may be radioactive, and neutrons.¹

Effective shielding for GCR is best accomplished by significantly reducing or eliminating the kinetic energy of the nuclei. This is done mainly through Coulombic interactions between the incoming GCR nucleus and electrons in the atoms of the shielding material. As the GCR nucleus impacts with the shielding material, it can transfer some of its energy to charged particles in the shield, slowing in the process. The more electrons present, the greater the ability to slow the GCR. Hydrogen, which has the highest number of electrons per unit mass, has been selected as the best material for shielding.

2) Neutrons:

Unlike other forms of radiation, neutrons are not ever-present, as their half-life is only about ten minutes. Rather, they are a product of interactions between other forms of radiation and the shielding materials. The danger posed by neutrons comes from the

possibility of absorption by atoms in equipment or biological systems to form unstable isotopes.

The production of neutrons through nuclear fission is a familiar topic in nuclear chemistry. A small fraction of the collisions between GCR and the shielding material results in nuclear fragmentation, thereby producing neutrons.

In order to reduce the danger of neutrons, species such as boron and gadolinium, which have high thermal neutron capture cross-sections, can be embedded in the shielding material. The neutron capture cross-section of a material is a measure of the probability that the material will absorb an available neutron and increases as the velocity of the neutron decreases. Both boron and gadolinium produce stable isotopes when they absorb neutrons. In addition to its role in protection against GCR, hydrogen is an important part of the neutron protection system as it helps to slow the neutrons, thereby increasing the probability of their absorption.

3)High-Energy Electromagnetic Radiation:

High-energy electromagnetic radiations can cause ionization, radical production, and bond cleavage when they interact with a molecule. This can cause extensive damage to structural, electrical, and biological materials. Those types of electromagnetic radiation with which we are most concerned are UV rays, X-rays, and gamma rays.

There are already well-established ways for guarding against UV radiation, including carbon black and other types of radiation-absorbing fillers.

Both gamma and X-ray photons can lose energy through Compton scattering, through the photoelectric effect, and through pair production. All three of these

processes are most likely to occur when the element with which the photons interact has a high atomic number. As a result, the best way to protect a spacecraft or a lunar or Martian habitat and its contents is through embedding high atomic number elements in the shielding material.

PROPOSED SOLUTION:

The problem of intensive radiation shielding in space travel is complicated by practical concerns such as weight limitations and feasibility of material construction. Lead or concrete might be candidates for blocking radiation, but launching a spacecraft made of those materials would be far too costly. A shield made of liquid hydrogen would be most effective against GCR, but maintaining such a material would be nearly impossible.

An ideal shielding material would be lightweight, strong, and thermally stable with high hydrogen content and would contain high atomic number elements with large neutron-capture cross sections. It would also be advantageous to have a material which could be incorporated into structural components of the habitat, thereby increasing the radiation shielding without adding unnecessary mass to the materials used to construct the habitat.

Polymers can be molded into a variety of shapes, making them potentially useful as structural features. By carefully choosing the monomer units involved in polymerization, the polymer can be tailor-made for a specific application. In this case, it is necessary to find a stable middle ground between structural integrity and radiation shielding capabilities.

Aliphatic polymers such as polyethylene and polypropylene have high hydrogen content (0.143 moles of hydrogen per gram of polymer in both cases). This high hydrogen content makes them the best polymers in regards to producing maximal Coulombic interactions for blocking GCR on a per gram basis. Unfortunately, the aliphatic nature of the backbone lends itself to poor mechanical and thermal properties necessary to withstand the extreme conditions present in outer space. Both thermal stability and mechanical strength can be increased by increasing the aromatic content of the polymer backbone.

High performance aromatic polymers provide an interesting route to the desired radiation shielding. While such materials are generally low in desired hydrogen content, they have desirable thermal and mechanical properties in comparison with their aliphatic counterparts. Kapton[®], a commercially available aromatic polyimide produced by DuPont[™], has a use range of -269°C to 400°C.² Polypropylene, on the other hand, has a service temperature of just -20°C to 175°C.³ The Young's modulus of Kapton[®] is 2.5 GPa and its tensile strength is 231 MPa.² For comparison, polypropylene's Young's modulus is 1.1-1.6 GPa and the tensile strength is 31-41 MPa.³ The aromatic polymers are to some extent tailorable in terms of their shielding capacity through careful selection or synthesis of monomer starting materials.

This research has explored (1) the production of nine novel aromatic compounds containing a hydrogen-rich cyclohexylene unit—three bisphenols and their dinitro and eventual diamine derivatives as candidate monomers; (2) the crystallographic structures of the bisphenol and dinitro compounds; (3) the preparation of aromatic polyimides of varying hydrogen content from these novel diamines.

BACKGROUND RESEARCH:

Polyimides

Properties:

Polyimides are, in many ways, perfect for this application. The compounds tend to have inherent radiation shielding properties⁴ to go along with their excellent thermal, mechanical, and chemical stabilities. Their excellent compressive strength and flexural modulus are maintained even at high temperatures⁵, allowing the materials to maintain their overall shape well under a variety of conditions. Polyimides are resistant to solvents, acids, and alkalis and are flame retardant.⁶ Additionally, as their poly(amic acid) precursors, polyimides can be molded into almost any form and can be made into useful composites.

Monomer Production:

1) Bisphenol Production:

The initial step in monomer production was bisphenol synthesis from a ketone and a phenol:

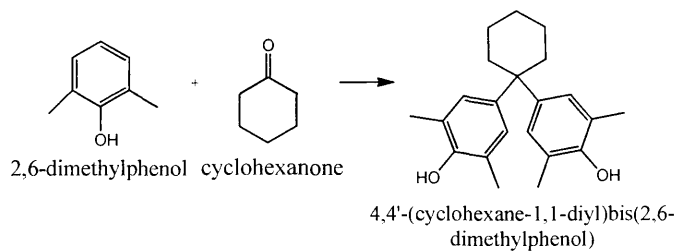


Figure (1): Bisphenol production from a ketone and a phenol.

Phenols were chosen for monomer precursors because of their aromatic character and the relative ease of reaction to form bisphenols. Additionally, bisphenols provide an

opportunity to produce a wide range of monomer precursors with varying levels of hydrogen content. Bisphenols were produced following a procedure by Weber, *et al.*⁷

A mechanism for this acid-catalyzed reaction was proposed by V. Braun in which the ketone and phenol create a *p*-isopropenylphenol intermediate.⁸ This mechanism is shown below where the ketone is acetone. A similar mechanism is likely in the bisphenol synthesis described here, where cyclohexanone is the ketone.

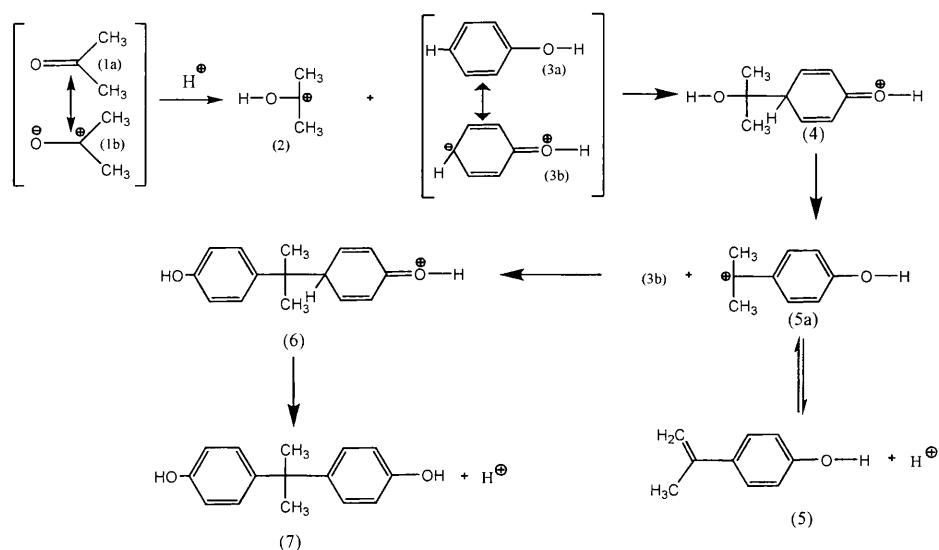


Figure (2): Mechanism for the reaction of a ketone (acetone) and a phenol.

A phenol and three different ketones with high hydrogen content were chosen for this study. Ketones generally, and cyclic ketones more specifically, were chosen over aldehydes and aliphatic acyclic ketones because of their increased reactivity in this context.⁸

2) Dinitro Production:

The three bisphenols were all converted to the dinitro compounds following a procedure outlined by Hu, *et al.*¹¹ The reaction is illustrated in Figure (3) for 5,5'-(cyclohexane-1,1-diyl)bis(1,3-dimethyl-2-(4-nitrophenoxy)benzene).

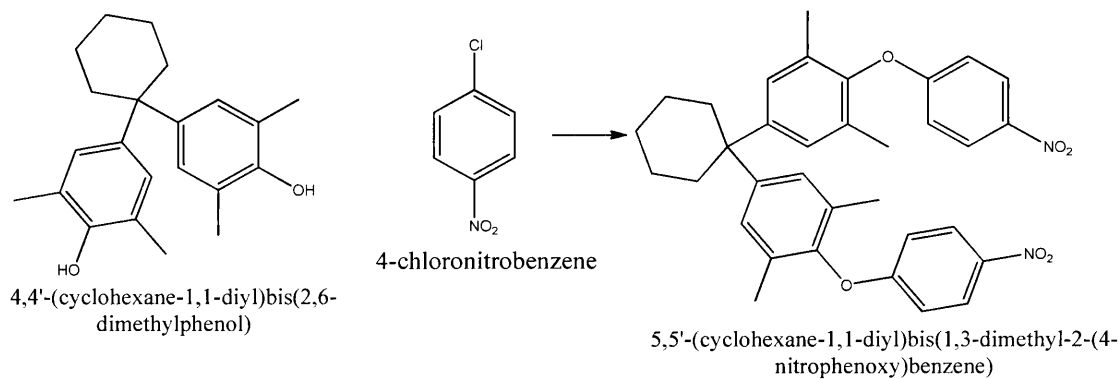


Figure (3): Synthesis of a dinitro compound from a bisphenol and 4-chloronitrobenzene.

This synthetic route was chosen because of the ease of converting the dinitro functionality into the desired diamine product.

3) Diamine Production:

Diamines were produced via hydrogenation, either through a procedure by Hu, *et al.*¹¹, or using a hydrogenation apparatus.¹² The reaction is illustrated in Figure (4) for the production of 4,4'-((cyclohexane-1,1-diyl)bis(2,6-dimethyl-4,1-phenylene))bis(oxy)dianiline.

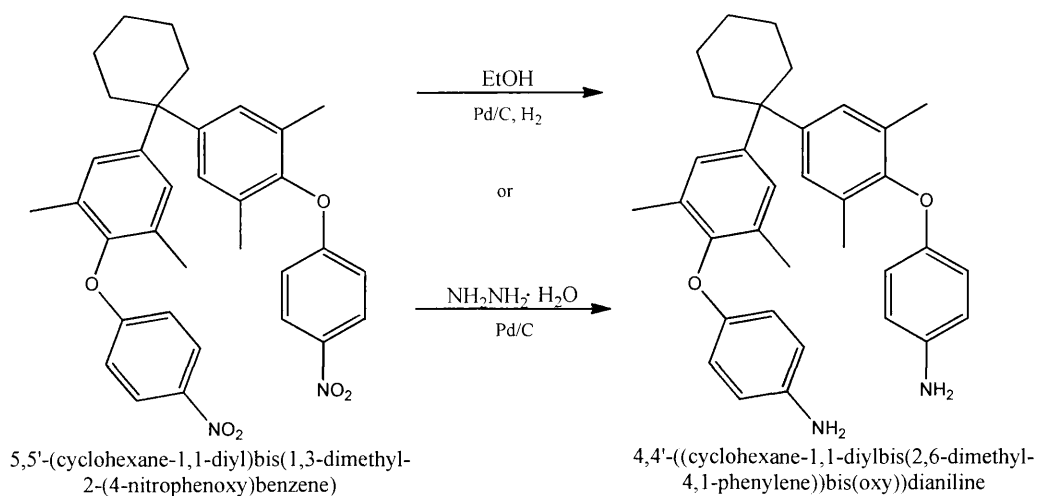


Figure (4): Diamine synthesis by hydrogenation of a dinitro compound.

Polymer Production:

Polyimides are most often produced in a two-step polymerization. The first step of the polymerization involves the step condensation of a diamine with a dianhydride to produce the poly(amic acid) precursor. The poly(amic acid) may then be converted to the final polymer through either thermal or through chemical dehydration.⁴ Generally polyimides are insoluble and cannot be softened below degradation temperatures for molding purposes. Because of the solvent resistance and high softening temperatures of polyimides, any efforts at forming a specific shape for the final polymer must take place before the final dehydration.

High molecular weight polymers can only be attained through careful attention to the correct stoichiometric ratio (in this case 1:1 diamine to dianhydride). Excess amounts of either monomer as a result of impurities or improper massing will result in low molecular weight polymers with decreased thermal and mechanical stability.

Additionally, the presence of monofunctionalized rather than difunctionalized monomer of either type will result in low molecular weight polymers through end-capping.

The polymerization mechanism is shown below:

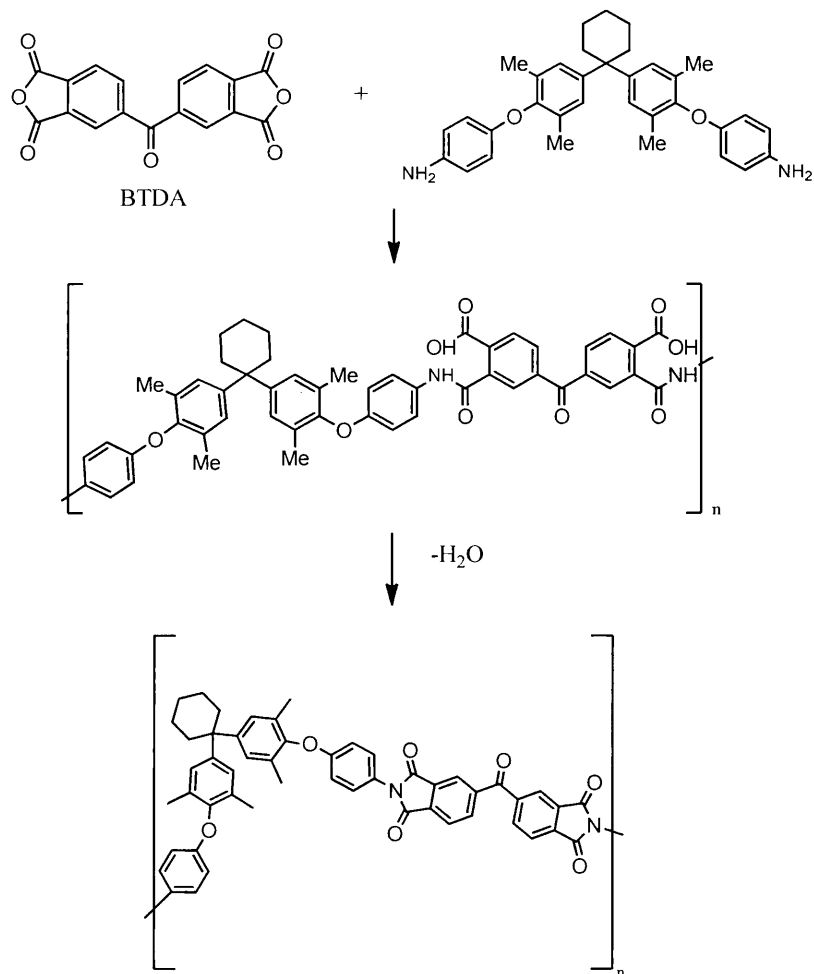


Figure (5): Polyimide synthesis using BTDA and TED monomers.

Benzophenone-3,3',4,4'-tetracarboxylic dianhydride (BTDA, structure shown above in Figure (5)) was selected for its preestablished suitability for polyimide synthesis, an application for which it is commonly used.

In this research, the polymers were cast as films, as they facilitate radiation shielding testing as well as providing the opportunity to explore the effects of layering and varying thicknesses. Ideally, the final product is a clear, bubble-free, creaseable film of even thickness. The ability of a film to be creased without cracking is used as a measure of high molecular weight. Any cloudiness, bubbles, or variations in thickness in the film interrupts the uniformity of the material, lowering its mechanical stability and causing variations in radiation shielding capabilities from one point to the next.

Gadolinium Modification:

Gadolinium is a heavy metal in the lanthanide series with atomic number $Z=64$ and a melting temperature of 1312°C . Isotopes of gadolinium span a mass range of 152-160 amu. Gadolinium's high atomic number makes it a good source of protection from high-energy electromagnetic radiation such as gamma rays and x-rays. Additionally, even with no isotopic enrichment, gadolinium has a high neutron capture cross section at 48.8×10^3 barns. For comparison, the neutron capture cross-section of carbon is 3.5 mb.¹⁰

In order to maximize the radiation shielding capabilities of the gadolinium, it is necessary to distribute the metal uniformly throughout the shielding material. Given the organic nature of the proposed polymeric shielding material and the solvent system used in polymerization, it seemed desirable to modify the gadolinium by creating its organic salt. Without said modification, the gadolinium clumps, reducing its utility in guarding against radiation.

In this research, the gadolinium was used as its phenyl acetate salt, produced through mixing a solution of gadolinium nitrate with a solution of phenyl acetic acid.

EXPERIMENTAL METHODS:

Materials:

All reactants were purchased from Sigma-Aldrich and, with the exception of the dianhydrides used in poly(amic acid) production, were used without further purification. Both the 4,4'-(4,4'-Isopropylidenediphenoxy)bis(phthalic anhydride) and 3,3',4,4'-benzophenone tetracarboxylic dianhydride were recrystallized using acetic anhydride. Solvents were purchased from Fisher Scientific.

Testing:

Purity was verified using a Varian 400 MHz Multi-nuclear NMR. Additionally, purity of diamines was assessed using thin layer chromatography. Melting temperatures were measured using a Mel-Temp device. Crystal structures were evaluated using a Bruker Smart APEX II X-ray Diffractometer.

Thermal properties of the polymer films were tested using a TA Instruments differential scanning calorimeter and a TA Q500 thermogravimetric analyzer.

Monomer Synthesis:

Bisphenol:

Three distinct bisphenols were produced through an acid-catalyzed reaction between 2,6-dimethylphenol and a cyclic ketone. See Figure (1). Their structures are shown below as Figure (6) a-c:

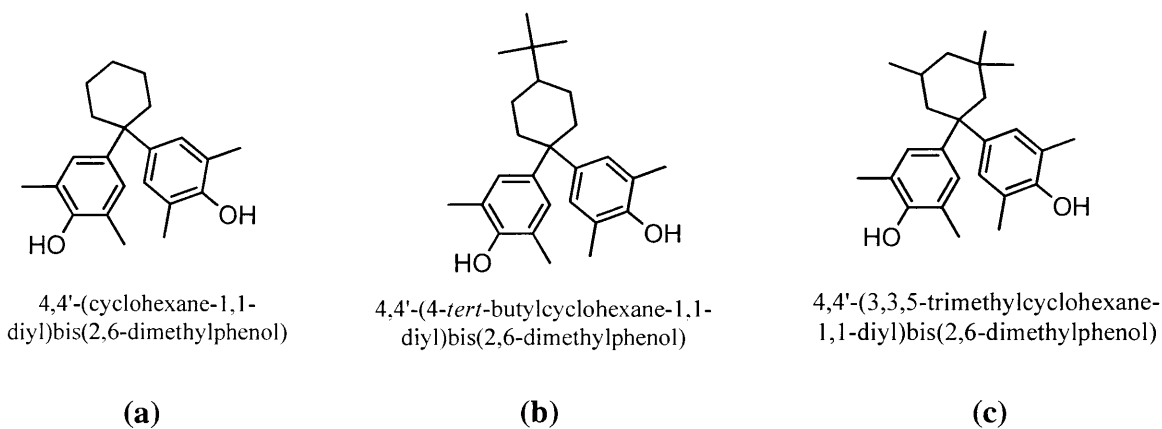


Figure (6): Bisphenol precursors.

1) Preparation of 4,4'-(cyclohexane-1,1-diyl)bis-2,6-dimethylphenol:

20 mL (0.19mol) of cyclohexanone and 114.53g (0.94mol) of 2,6-dimethylphenol were combined and then added dropwise to a solution of 38mL concentrated glacial acetic acid, 20mL concentrated sulfuric acid, and 0.5mL dimethyl sulfoxide at 0°C. The reaction was allowed to continue at constant temperature for 90 minutes, producing a brown sludge. The reaction mixture was then precipitated in 0.5L of water and heated to 30°C, whereupon the mixture turned blue. The solids were then collected by vacuum filtration and the filtrate (consisting of water and a blue/purple oil) was discarded. The solids were deposited into a solution of 250mL distilled water and 1.25g sodium acetate and heated to 90°C with stirring. The solids became a pinkish brown sludge, which was then allowed to cool to room temperature before being filtered by suction and recrystallized using chlorobenzene. The recrystallization yielded a white crystal with a melting point of 200-202°C.

This procedure has been detailed in previous work.¹³ The crystal structure was obtained for this compound and is shown as Figure (9) a-b. Crystallographic data are

detailed in Appendix I. The proton-NMR assignments are as follows: $^1\text{H-NMR}$ (CDCl_3): δ (ppm) = 1.52 (m, 6H, CH_2), 2.2 (m, 16H, CH_2 , CH_3), 4.42 (s, 2H, OH), 6.86 (s, 4H, Ar-H).

2) Preparation of 4,4'-(4-*tert*-butylcyclohexane-1,1-diyl)bis(2,6-dimethylphenol):

Preparation of this compound was accomplished following the above procedure with the following alterations: 4-*tert*-butylcyclohexanone was used in place of cyclohexanone. Because of the lowered solubility of the ketone/phenol mixture, the glacial acetic acid was added to the ketone and phenol rather than being combined with the sulfuric acid and DMSO in the reaction flask. Additionally, the reaction was allowed to continue overnight, producing a red sludge.

Workup and purification were carried out as described above, resulting in a white or off-white crystal (m.p.=223-226°C). Similarly to the procedure above, this synthesis has already been detailed.¹³ The crystal structure for this compound is shown as Figure (10) a-b below. Crystallographic data are given in Appendix I. The $^1\text{H-NMR}$ spectrum is consistent with the chemical structure of this bisphenol: $^1\text{H-NMR}$ peaks (DMSO): δ (ppm) = 0.706 (s, 9H, CH_3), 1.577 (s, 4H, Cyclic- CH_2), 2.067 (m, 12H, Ar- CH_3), 2.475 (m, 5H, Cyclic- CH_2 , Cyclic-CH), 2.62 (s, 2H, OH), 6.67 (d, 2H, Ar-H), 6.83 (d, 2H, Ar-H).

3) Preparation of 4,4'-(3,3,5-trimethylcyclohexane-1,1-diyl)bis(2,6-dimethylphenol):

4,4'-(3,3,5-trimethylcyclohexane-1,1-diyl)bis(2,6-dimethylphenol) was prepared in a method identical to that used to produce 4,4'-(4-*tert*-butylcyclohexane-1,1-diyl)bis(2,6-dimethylphenol) excepting that 3,3,5-trimethylcyclohexanone was used in place of 4-*tert*-butylcyclohexanone and that this reaction was allowed to continue for up to three weeks to ensure adequate yields of product. The initial recrystallization yielded a white powder (m.p.=236-237°).

The crystal structure of this bisphenol was verified using a Bruker X-ray Diffractometer (see Figure (11) a-b) following evaporative crystallization from ethanol (see Appendix I for crystallographic data). Additionally, the proton-NMR structure is as follows: ¹H-NMR (DMSO): δ (ppm) = 0.298 (s, 3H, CH₃), 0.902 (s, 6H, CH₃), 1.23 (d, 1H, cyclic CH), 1.65 (d, 1H, cyclic CH₂), 1.82 (m, 1H, cyclic CH), 2.05 (m, 3H, cyclic CH, 12H, Ar-CH₃), 2.4 (d, 1H, cyclic CH), 3.3 (s, 2H, OH), 6.69 (s, 2H, Ar-H), 6.81 (s, 2H, Ar-H).

Dinitro:

All three bisphenols were successfully converted to their dinitro derivatives. The structures of these derivatives are shown below as Figure (7) a-c.

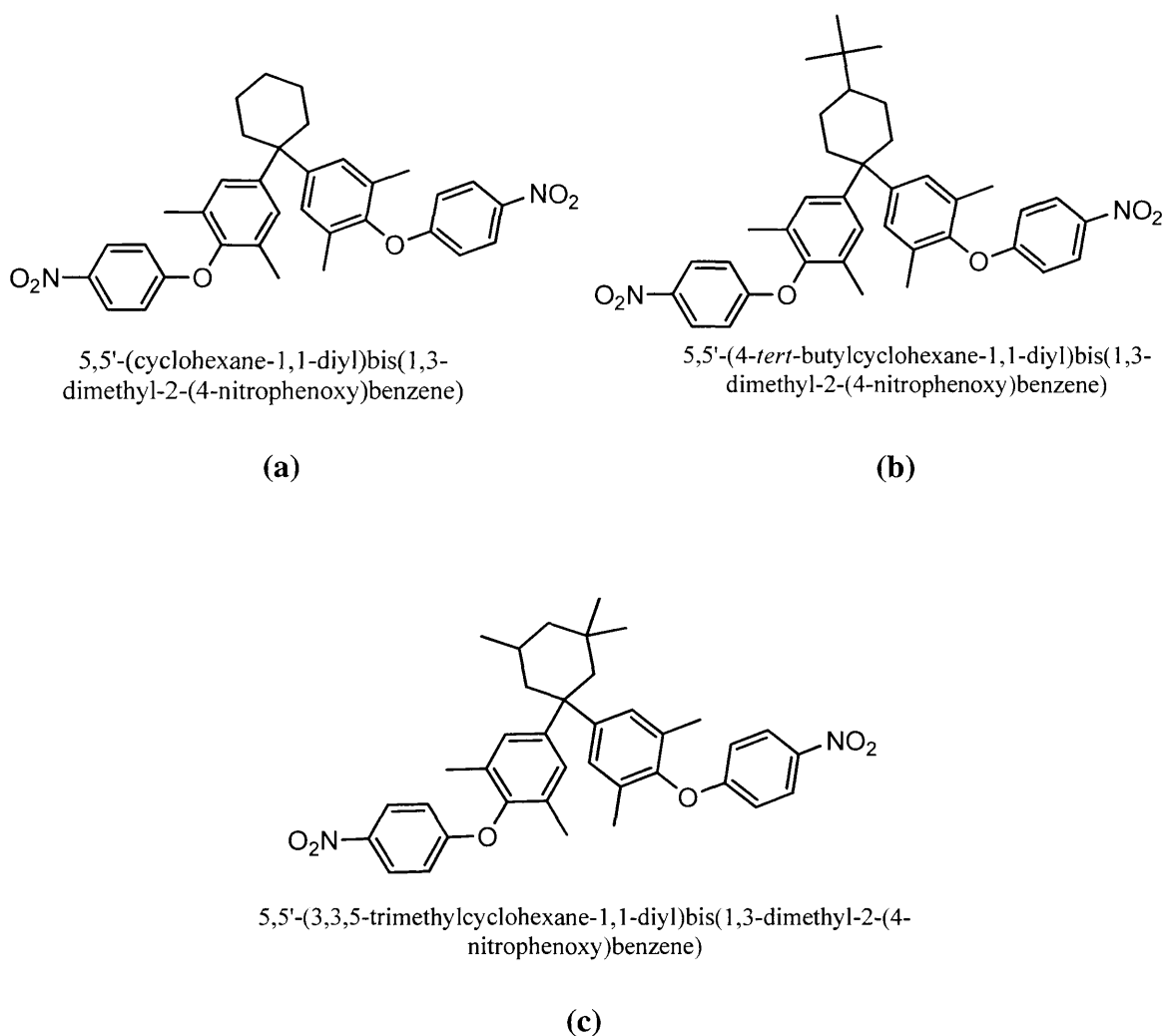


Figure (7): Dinitro precursors.

1) Synthesis of 5,5'-(cyclohexane-1,1-diyl)bis(1,3-dimethyl-2-(4-nitrophenoxy)benzene):

5,5'-(cyclohexane-1,1-diyl)bis(1,3-dimethyl-2-(4-nitrophenoxy)benzene) was prepared from its bisphenol precursor through a procedure modeled by Hu, *et al.*¹¹ 24.98g (0.077 mol) of 4,4'-(cyclohexane-1,1-diyl)bis-2,6-dimethylphenol was combined in a reaction flask with 26g (0.166 mol) of 4-chloronitrobenzene in the

presence of 25.133g (0.184 mol) potassium carbonate and 116 mL dimethylformamide (DMF) and refluxed overnight at 170°C.

The resulting greenish-black mixture was then poured onto two liters of a 1:1 v/v methanol to water solution, causing the formation of a yellow precipitate. This precipitate was then filtered by suction and recrystallized from glacial acetic acid. The recrystallization required extremely slow cooling to ensure that adequate purity is attained before attempting the next step.

Recrystallization resulted in flat brown-orange crystals with a melting temperature of 192°C, the structure of which was verified using x-ray diffraction techniques (see Figure (12) a-c for an illustration and Appendix I for crystallographic data). The ¹H-NMR data are consistent with the structure of this compound as shown in Figure (7)a: ¹H-NMR peaks (CDCl₃): δ (ppm) = 1.6 (d, 6H, cyclic-CH₂), 2.1 (t, 12H, Ar-CH₃), 2.25 (s, 4H, cyclic CH₂), 6.8 (d, 4H, Ar-H), 7.05 (t, 4H, Ar-H), 8.1 (d, 4H, Ar-H).

2) Synthesis of 5,5'-(4-*tert*-butylcyclohexane-1,1-diyl)bis(1,3-dimethyl-2-(4-nitrophenoxy)benzene):

This dinitro compound was initially synthesized in a manner identical to that described above. Following gas chromatographic testing it was found that the 4-chloronitrobenzene did not completely add to both sides. In order to ensure adequate addition, excess chloronitrobenzene was added to the reaction mixture.

In this reaction 26.7098g (0.0729mol) 4,4'-(4-*tert*-butylcyclohexane-1,1-diyl)bis(2,6-dimethylphenol) was combined with 35g (0.222mol) 4-chloronitrobenzene and 23.792g (0.172mol) potassium carbonate in 109.4 mL DMF. The reaction mixture

was allowed to reflux overnight at 165°C. Precipitation and recrystallization were carried out as described above.

The reaction resulted in yellow-brown crystals (see Appendix I for crystallographic data and Figure (13) a-b for an illustration of crystal structure) with a melting temperature of 207°C. ¹H-NMR data are consistent with this compound's chemical structure: ¹H-NMR (CDCl₃): δ (ppm) = 0.8 (s, 9H, CH₃), 1.2 (m, 4H, cyclic CH₂), 1.7 (d, 2H, cyclic CH₂, 1H cyclic CH), 1.9 (t, 2H, cyclic CH₂), 2.05 (s, 6H, Ar-CH₃), 2.1 (s, 6H, Ar-CH₃), 2.7 (d, 2H, cyclic CH₂), 6.81 (doublet of doublets, 4H, Ar-H), 6.94 (s, 2H, Ar-H), 7.12 (s, 2H, Ar-H), 8.17 (m, 4H, Ar-H).

3) Synthesis of 5,5'-(3,3,5-trimethylcyclohexane-1,1-diyl)bis(1,3-dimethyl-2-(4-nitrophenoxy)benzene):

5,5'-(3,3,5-trimethylcyclohexane-1,1-diyl)bis(1,3-dimethyl-2-(4-nitrophenoxy)benzene) was synthesized in a manner identical to the procedure for synthesizing 5,5'-(4-*tert*-butylcyclohexane-1,1-diyl)bis(1,3-dimethyl-2-(4-nitrophenoxy)benzene) excepting, of course, the use of 4,4'-(3,3,5-trimethylcyclohexane-1,1-diyl)bis(2,6-dimethylphenol) in place of 4,4'-(4-*tert*-butylcyclohexane-1,1-diyl)bis(2,6-dimethylphenol).

Recrystallization resulted in a yellow-orange crystal (see Figure (14) a-b for an illustration and Appendix I for crystallographic data) with a melting temperature of 148°C. As discussed below, acetic acid co-precipitated with the bisphenol in a 1:1 molar ratio. ¹H-NMR data are consistent with the compound's chemical structure: ¹H-NMR (CDCl₃): δ (ppm) = 0.43 (s, 3H, CH₃), 0.90 (t, 1H, cyclic CH₂), 1.02 (2 overlapped s, 6H,

CH₃), 1.17 (t, 1H, cyclic CH₂), 1.42 (d, 1H, cyclic CH), 1.93 (d, 2H, cyclic CH₂), 2.05 (s, 6H, Ar-CH₃), 2.08 (s, 6H, Ar-CH₃), 2.48 (d, 1H, cyclic CH₂), 2.70 (d, 1H, cyclic CH₂), 6.80 (q, 4H, Ar-H), 6.98 (s, 2H, Ar-H), 7.10 (s, 2H, Ar-H), 8.16 (q, 4H, Ar-H).

Diamine:

Each of the above listed dinitro compounds was in turn converted to its diamine derivative. Structures are illustrated below as Figure (8) a-c:

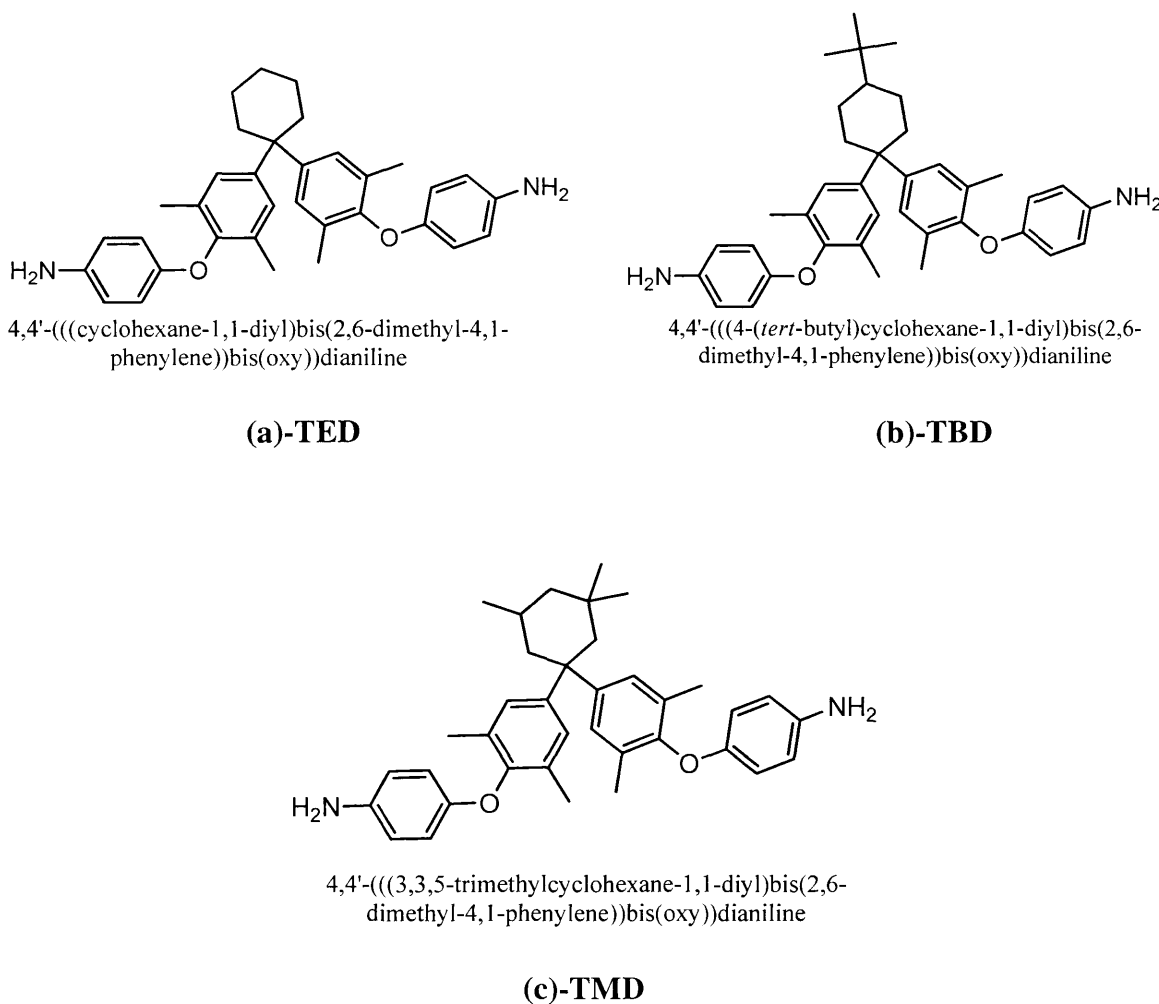


Figure (8): Diamine monomers.

1) Synthesis of 4,4'-(((4,4'-cyclohexane-1,1-diyl)bis(2,6-dimethyl-4,1-phenylene))bis(oxy))dianiline:

4,4'-(4,4'-cyclohexane-1,1-diyl)bis(2,6-dimethyl-4,1-phenylene))bis(oxy) dianiline (hereafter referred to as TED) was synthesized via two distinct methods. The first of these was carried out according to a procedure by Hu, *et al.*¹¹ A solution consisting of 54.9813g of 4,4'-(cyclohexane-1,1-diyl)bis(1,3-dimethyl-2-(4-nitrophenoxy)benzene), 259mL of ethanol, and 0.3877g of 10%Pd on active carbon was placed in a three necked flask and heated to 85°C. 193.7mL of hydrazine monohydrate was then added drop-by-drop to the reaction flask. The reaction was allowed to continue for a full day at reflux. The solution was then hot filtered to remove the palladium catalyst. The diamine was precipitated using ice and collected by vacuum filtration.

The second method for synthesis of TED utilized a hydrogenation apparatus¹² to which was attached a 500mL reinforced bottle containing ethanol, 4,4'-(cyclohexane-1,1-diyl)bis(1,3-dimethyl-2-(4-nitrophenoxy)benzene), and a 10% Pd on active carbon catalyst was attached. The reaction vessel was then charged up to 50 psi of hydrogen gas and allowed to react overnight. Details for this reaction are given elsewhere.¹³ The palladium catalyst was removed by filtration before the product was collected by evaporation of solvent using a Roto-Vap apparatus. The diamine was then dissolved in ethyl acetate and dried first under nitrogen and then under vacuum.

¹H-NMR data are consistent with the diamine structure: ¹H-NMR (CDCl₃): δ (ppm) = 1.50 (br. t, 6H, cyclic CH₂), 2.08 (s, 12H, Ar-CH₃), 2.23 (br. t, 4H, cyclic CH₂), 3.41 (br. s, 4H, NH₂), 6.57 (m, 8H, Ar-H), 6.95 (s, 4H, Ar-H).

2) Synthesis of 4,4'-(((4-(*tert*-butyl)cyclohexane-1,1-diyl)bis(2,6-dimethyl-4,1-phenylene))bis(oxy))dianiline:

The synthesis of 4,4'-(((4-(*tert*-butyl)cyclohexane-1,1-diyl)bis(2,6-dimethyl-4,1-phenylene))bis(oxy))dianiline (hereafter referred to as TBD) was accomplished following both procedures listed above. In both cases, 5,5'-(4-*tert*-butylcyclohexane-1,1-diyl)bis(1,3-dimethyl-2-(4-nitrophenoxy)benzene) was used in place of 4,4'-(cyclohexane-1,1-diyl)bis(1,3-dimethyl-2-(4-nitrophenoxy)benzene).

¹H-NMR data are consistent with the diamine's structure: ¹H-NMR (CDCl₃): δ (ppm) = 0.80 (s, 9H, CH₃), 1.18 (t, 2H, cyclic CH₂), 1.70 (d, 2H, cyclic CH₂), 1.87 (t, 2H, cyclic CH₂, 1H, cyclic CH), 2.05 (s, 6H, Ar-CH₃), 2.12 (s, 6H, Ar-CH₃), 2.68 (d, 2H, cyclic CH₂), 3.40 (br. s, 4H, NH₂), 6.57 (m, 8H, Ar-H), 6.87 (s, 2H, Ar-H), 7.06 (s, 2H, Ar-H).

3) Synthesis of 4,4'-(((3,3,5-trimethylcyclohexane-1,1-diyl)bis(2,6-dimethyl-4,1-phenylene))bis(oxy))dianiline:

4,4'-(((3,3,5-trimethylcyclohexane-1,1-diyl)bis(2,6-dimethyl-4,1-phenylene))bis(oxy))dianiline (also referred to as TMD) was synthesized using the hydrogenation apparatus with 5,5'-(3,3,5-trimethylcyclohexane-1,1-diyl)bis(1,3-dimethyl-2-(4-nitrophenoxy)benzene) in place of 4,4'-(cyclohexane-1,1-diyl)bis(1,3-dimethyl-2-(4-nitrophenoxy)benzene).

¹H-NMR was consistent with the compound's chemical structure: ¹H-NMR (CDCl₃): δ (ppm) = 0.42 (s, 3H, CH₃), 0.88 (t, 2H, cyclic CH₂), 1.00 (2 overlapped s, 6H, CH₃), 1.15 (q, 1H, cyclic CH₂), 1.40 (d, 1H, cyclic CH₂), 2.06 (s, 6H, Ar-CH₃), 2.10 (s,

6H, Ar-CH₃), 2.16 (m, 1H, cyclic CH), 2.46 (d, 1H, cyclic CH₂), 2.69 (d, 1H, cyclic CH₂), 3.40 (br. s, 4H, NH₂), 6.56 (m, 8H, Ar-H), 6.92 (s, 2H, Ar-H), 7.04 (s, 2H, Ar-H).

Diamine Purification:

Initial attempts at diamine synthesis resulted in impure product, as verified by thin-layer chromatography. In order to obtain an ¹H-NMR spectrum to which later samples could be compared, small portions of the impure diamine samples were subjected to column chromatography. Silica gel was utilized as the stationary phase while the eluent was composed of a 2:1 mixture of ethyl acetate and hexanes.¹⁴

Dianhydride Purification:

3,3',4,4'-benzophenone tetracarboxylic dianhydride (BTDA) was obtained from Sigma Aldrich at 96% purity. In order to obtain adequate purity for polymerization, the BTDA was recrystallized using acetic anhydride. Purity was assessed by Melt-Temp apparatus. Directly out of the bottle the melting temperature spanned 219-222°C. Following recrystallization, the melting occurred at 224°C.

Polyimide Synthesis:

1) TED/BTDA:

TED and 3,3',4,4'-benzophenone tetracarboxylic dianhydride (BTDA) were reacted in the presence of NMP to form a polyimide.

The first step was the synthesis of the poly(amic acid). Under nitrogen and in an ice bath, 1.8338g (0.003619 mol) TED was dissolved in 8.953g (8.709mL) NMP to

create a 17% by weight solution. Separately, 1.1662g (0.003619 mol) BTDA was combined in 5.6938g (5.5387mL) NMP to make another 17% by weight solution. Once both compounds were fully dissolved, the dianhydride solution was added dropwise to the diamine solution. The reaction mixture was maintained in an ice bath for three to four hours before being allowed to come up to room temperature. The polymerization was allowed to continue overnight.

An alternate, but nearly identical synthetic procedure was also used. In this case, after the diamine was completely dissolved in its portion of NMP, the BTDA was added as a solid and followed immediately by its portion of NMP.

In either case, the second step in the polyimide synthesis was carried out the following day. A glass plate was placed in a base bath (consisting of 130g potassium hydroxide tablets dissolved in 7.87L isopropanol and 2.00L deionized water) for at least an hour to ensure a clean surface. The plate was then cleaned with detergent, rinsed first with water, then acetone, and finally with ethanol before being allowed to dry completely. Once the plate was dry, a doctor blade was set to 0.635mm. The poly(amic acid) was then poured onto the plate in a straight line and pulled at a right angle to the line to uniform thickness. The coated plate was then placed in a programmable oven and heated to 300°C in four steps. It was heated to 100°C, then to 200°C, then to 250°C, and finally to 300°C at a rate of 100°C/hr for each set point. The oven was held isothermally for an hour at each temperature. After cooling to room temperature, the film was removed from the glass plate by placing the plate in a water bath.

2) TBD/BTDA:

A polymer was made from TBD and BTDA in a manner identical to that for the TED/BTDA polymer with the exception that the relative masses of the diamine and dianhydride had to be altered to compensate for the differences in molecular weight between TED and TBD. In synthesizing the TBD/BTDA polymer, 1.9077g (0.003390 mol) TBD was dissolved in 9.3140g (9.0610mL) NMP and 1.0923g (0.003390mol) BTDA was dissolved in 5.3340g (5.1880mL) NMP. The alternate procedure in which the BTDA was added as a solid was also attempted with the TBD/BTDA polymer. In both cases, the remainder of the procedure was identical to that for TED/BTDA.

3) TMD/BTDA:

Attempts were made at producing a polymer from TMD and BTDA using both procedures described above. Both procedures were carried out as described above, excepting alterations required by differences in molecular weight of the diamine. 1.8901g (0.003444mol) TMD was dissolved in 9.2283g (8.9770mL) NMP and 1.1099g (0.003444mol) BTDA was combined with 5.4187g (5.2711mL) NMP.

4) TED/UDA:

A polymer was attempted following an identical procedure as detailed above using 4,4'-(4,4'-Isopropylidenediphenoxy)bis(phthalic anhydride) (UDA) in place of the BTDA. 1.5202g (0.002920mol) UDA was dissolved in 8.9421g (8.6986mL) NMP before being added to a solution of 1.4798g (0.002920mol) TED in 8.7049g (8.4678mL) NMP.

The resulting polymer was brittle and fragmented when removed from the oven. No thermal characterizations were carried out.

5) TBD/UDA:

A polymer consisting of TBD and UDA was also attempted. In this case 1.4414g (0.002769mol) UDA was dissolved in 8.4790g (8.2481mL) NMP and added dropwise to a solution of 1.5586g (0.002769mol) TBD in 9.1681g (8.9183mL) NMP.

As with the TED/UDA film, this film was fragmented when removed from the oven. No characterizations were attempted.

Gadolinium Salt Production:

Gadolinium phenyl acetate was produced following a procedure outlined in Harbert, 2010.¹⁵

7.2558g of phenyl acetic acid was dissolved in 500mL of water. The pH of the solution was then adjusted to 5 by dropwise addition of ammonium hydroxide. Simultaneously, 8.0213g of gadolinium nitrate was dissolved in another 300mL of water. Under stirring, the gadolinium nitrate solution was added slowly to the phenyl acetic acid solution, leading to the formation of a white precipitate. The precipitate was then collected by vacuum filtration and dried in an oven at 120°C for three days.

The salt was then sent to Atlantic Microlab, Inc for elemental analysis.

RESULTS AND DISCUSSION:

Bisphenol Monomer:

All three bisphenol monomers were produced and characterized by $^1\text{H-NMR}$ in previous research.¹³ All three bisphenol monomers were characterized by single-crystal X-ray diffraction. Illustrations of their structures and packing are shown below. 4,4'-(cyclohexane-1,1-diyl)bis-2,6-dimethylphenol appears as Figure (9) a-b, 4,4'-(4-*tert*-butylcyclohexane-1,1-diyl)bis(2,6-dimethylphenol) appears as Figure (10) a-b, and 4,4'-(3,3,5-trimethylcyclohexane-1,1-diyl)bis(2,6-dimethylphenol) appears as Figure (11) a-b. Crystallographic data for all three compounds appears in Appendix I.

For 4,4'-(cyclohexane-1,1-diyl)bis-2,6-dimethylphenol, recrystallization from chlorobenzene sufficed to produce crystals of a quality appropriate for X-ray diffraction. For both 4,4'-(4-*tert*-butylcyclohexane-1,1-diyl)bis(2,6-dimethylphenol) and 4,4'-(3,3,5-trimethylcyclohexane-1,1-diyl)bis(2,6-dimethylphenol), it was necessary to carry out evaporative crystallization from ethanol to produce useful crystals.

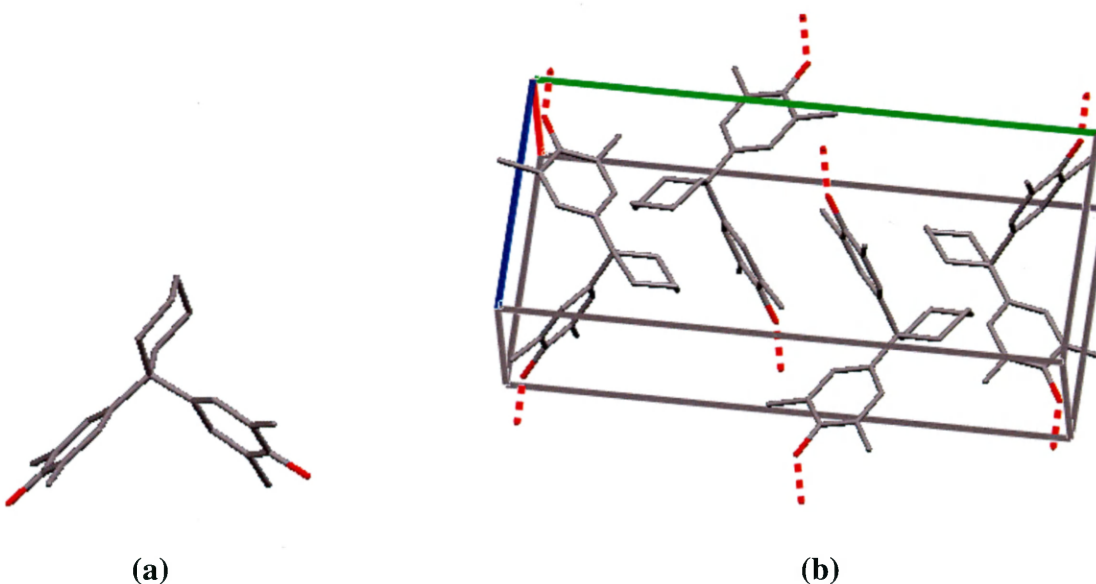


Figure (9): TED bisphenol crystal structure

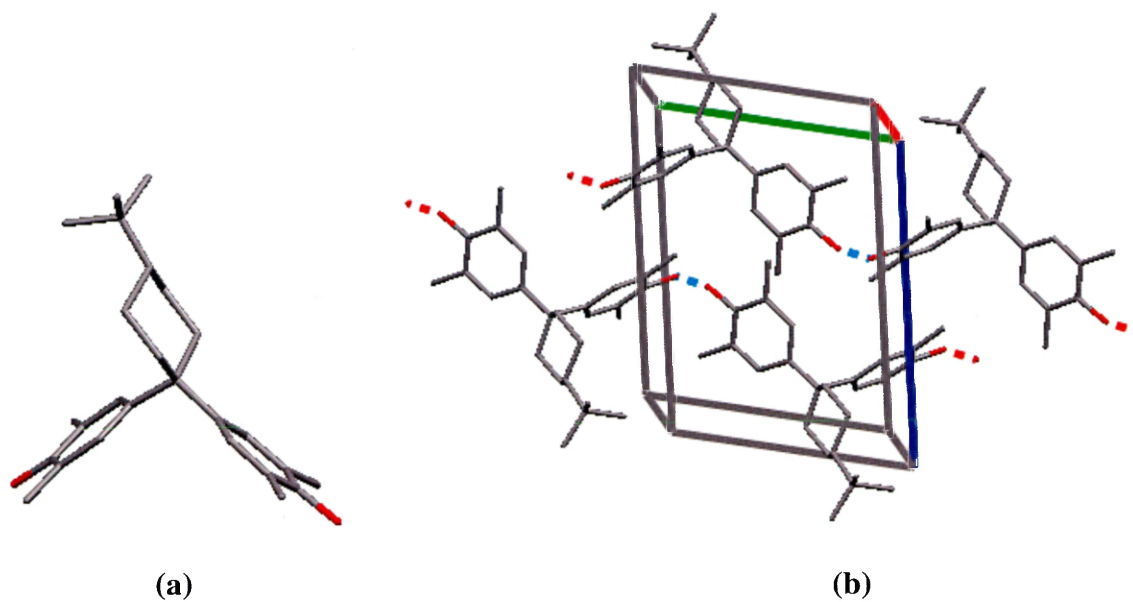


Figure (10): TBD bisphenol crystal structure.

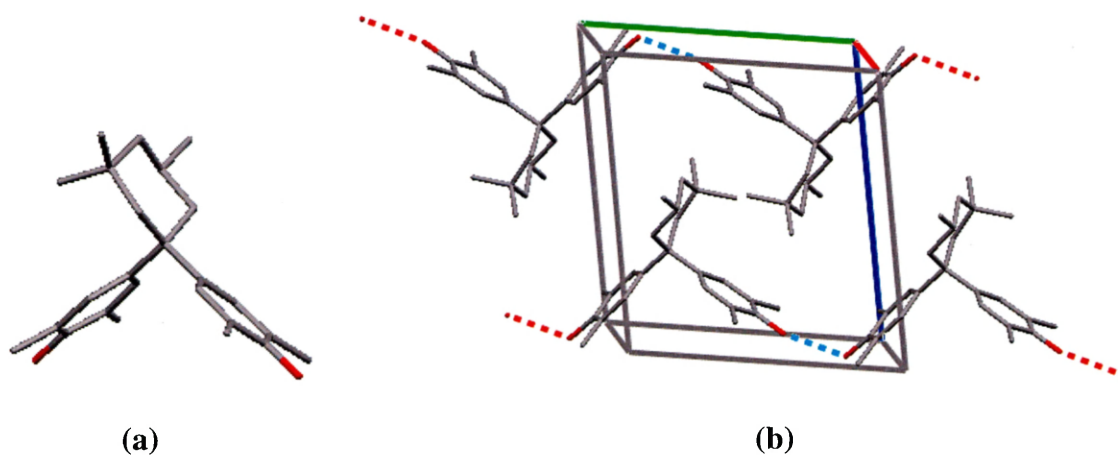


Figure (11): TMD bisphenol crystal structure.

Dinitro Production and Purification:

Both 5,5'-(cyclohexane-1,1-diyl)bis(1,3-dimethyl-2-(4-nitrophenoxy)benzene) and 5,5'-(4-*tert*-butylcyclohexane-1,1-diyl)bis(1,3-dimethyl-2-(4-nitrophenoxy)benzene) were produced in previous research.¹³ Better purification techniques in the production of

4,4'-(3,3,5-trimethylcyclohexane-1,1-diyl)bis(2,6-dimethylphenol) led to the production of 5,5'-(3,3,5-trimethylcyclohexane-1,1-diyl)bis(1,3-dimethyl-2-(4-nitrophenoxy)benzene). The structures of all three compounds were explored using ^1H -NMR and single-crystal X-ray diffraction.

Initial purification of the dinitro derivatives was carried out by recrystallization using glacial acetic acid. Efficient recrystallization of the crude product requires that the crude product be dry before addition of any acetic acid. Adequate drying was accomplished by continuing to pull air over the sample at room temperature for two hours following vacuum filtration.

Extensive difficulty in producing high molecular weights in the subsequent polymerization was attributed to impurities in the diamine. Consequently, the purity of the dinitro precursors to the diamine compounds was revisited. Extended cooling times during recrystallization proved the most successful route for improving dinitro—and eventual diamine—purity. A programmable oven was used to decrease the temperature of the recrystallization mixture from 118°C to room temperature (roughly 23°C) at a rate of 0.1°C/minute. Not only did this increase purity of the dinitro compound in all three cases, it produced excellent crystals, which were then evaluated using single-crystal diffraction techniques.

Crystal structures of all three dinitro compounds are shown below along with illustrations of their packing formations. 5,5'-(cyclohexane-1,1-diyl)bis(1,3-dimethyl-2-(4-nitrophenoxy)benzene) is shown as Figure (12) a-c, 5,5'-(4-*tert*-butylcyclohexane-1,1-diyl)bis(1,3-dimethyl-2-(4-nitrophenoxy)benzene) is shown as Figure (13) a-b, and 5,5'-

(3,3,5-trimethylcyclohexane-1,1-diyl)bis(1,3-dimethyl-2-(4-nitrophenoxy)benzene) is shown as Figure (14) a-b.

5,5'-(cyclohexane-1,1-diyl)bis(1,3-dimethyl-2-(4-nitrophenoxy)benzene) displays two different structural orientations in its crystal structure, shown below as Figures (12) a-b.

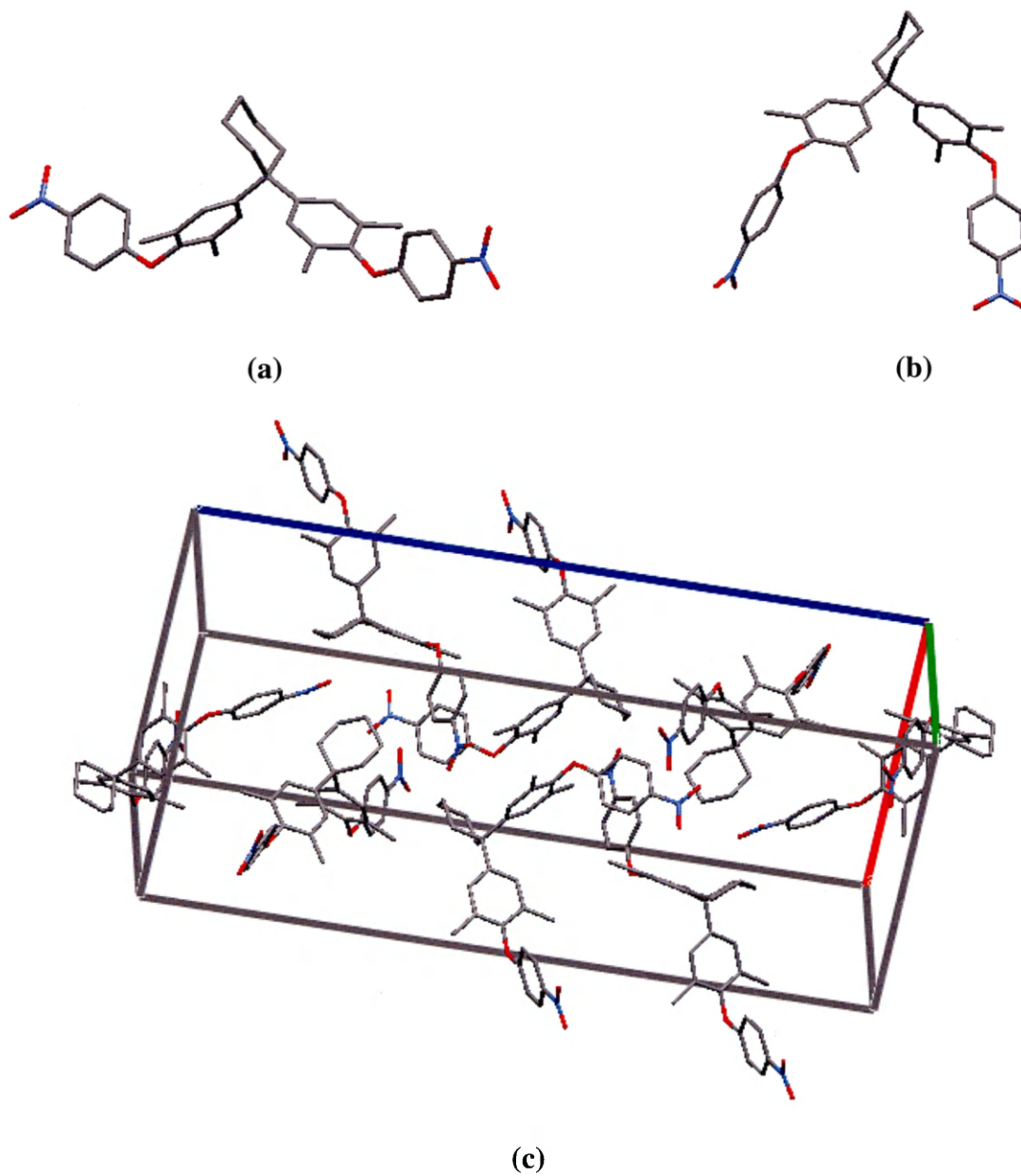


Figure (12): TED dinitro crystal structure.

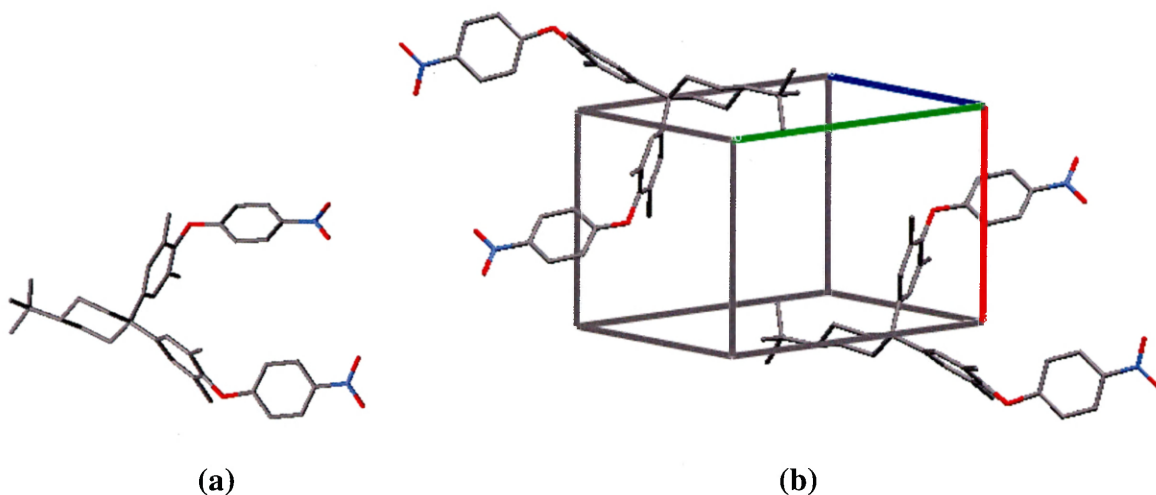


Figure (13): TBD dinitro crystal structure.

The packing of 5,5'-(3,3,5-trimethylcyclohexane-1,1-diyl)bis(1,3-dimethyl-2-(4-nitrophenoxy)benzene) includes acetic acid—a molecule of acetic acid for every molecule of dinitro compound—which crystallized with the dinitro compound.

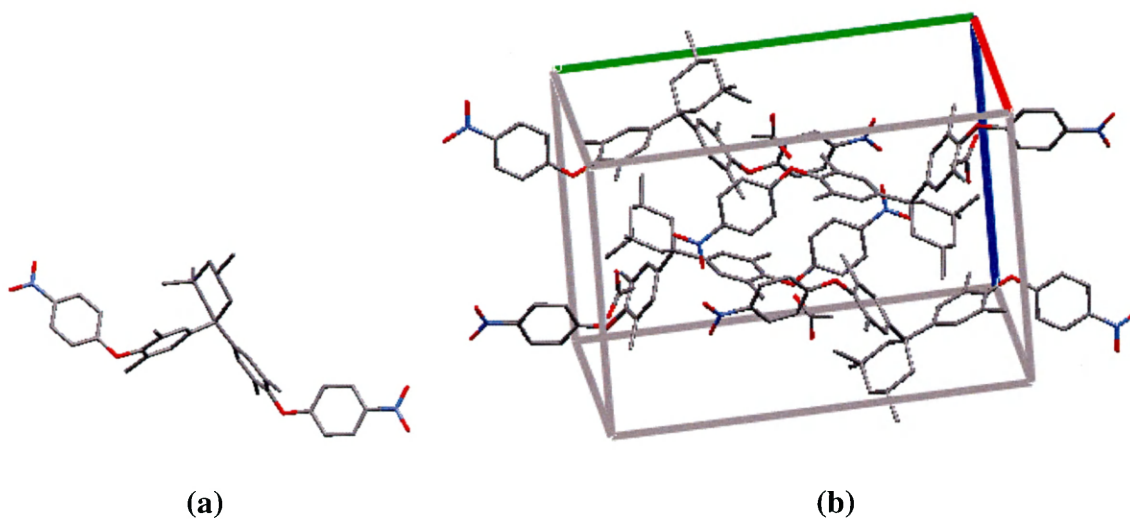


Figure (14): TMD dinitro crystal structure.

Diamine Production:

4,4'-(4,4'-(cyclohexane-1,1-diyl)bis(2,6-dimethyl-4,1-phenylene))bis(oxy)dianiline was successfully synthesized in previous work.¹³ Both 4,4'-(4,4'-(4-*tert*-butylcyclohexane-1,1-diyl)bis(2,6-dimethyl-4,1-phenylene))bis(oxy)dianiline and 4,4'-(((3,3,5-trimethylcyclohexane-1,1-diyl)bis(2,6-dimethyl-4,1-phenylene))bis(oxy))dianiline were successfully synthesized in the course of this research. ¹H-NMR characterization of the latter two diamines was problematic because of the lack of symmetry in the molecules which results in uncertain overlap in ¹H-NMR spectra.

Verification of structure was sought using LC-MS to explore molecular weights of the synthesized diamines. The analyses suggested complete purity of the diamines. However, attempts at polymerization with each one of the three diamines produced low molecular weight polymers which cracked upon removal from the curing plates. In the best case, the polymer films remained intact upon removal from the plate, but cracked when tested for creasability.

In response to the films' lack of creasability, the diamines were each subjected to thin-layer chromatography (TLC) in a 6:4 mixture of ethyl acetate to hexanes. The TLC plates showed extensive impurities, with the desired product appearing as the bottom-most spot. This spot was stainable in potassium permanganate in all three cases.

Following the TLC tests, the diamines were each purified using column chromatography. A silica gel adsorbent was utilized with a 2:1 ethyl acetate to hexanes eluent. In all three cases, small volumes of pure diamine were obtained and then characterized using ¹H-NMR.

While column chromatography seems to be the most certain way of ensuring diamine purity, it is far from being efficient in large-scale production. In light of this, and in light of the fact that the hydrogenation procedure should not produce side products, it was decided that purity of the diamine could best be accomplished by amply purifying the dinitro precursor, as detailed in the previous section. It was also decided that following synthesis the diamine must be isolated and stored in such a way as to prevent oxidation.

In an attempt to further guard the purity of the diamine, the precipitation step in diamine production was discarded in favor of solvent evaporation using a Rotovap apparatus. The compound was then collected with pure ethyl acetate and dried, first under nitrogen and then under vacuum.

When there was acetic acid present in the dinitro compound used in production of 4,4'-(4,4'-(cyclohexane-1,1-diyl)bis(2,6-dimethyl-4,1-phenylene))bis(oxy)dianiline, the resulting diamine, though apparently pure, appeared as a dark viscous fluid and was exceedingly difficult to dry. If the dinitro precursor had been adequately dried, however, 4,4'-(4,4'-(cyclohexane-1,1-diyl)bis(2,6-dimethyl-4,1-phenylene))bis(oxy)dianiline was a pinkish chalky solid.

This difference may also be true of 4,4'-(4,4'-(4-*tert*-butylcyclohexane-1,1-diyl)bis(2,6-dimethyl-4,1-phenylene))bis(oxy)dianiline and 4,4'-(((3,3,5-trimethylcyclohexane-1,1-diyl)bis(2,6-dimethyl-4,1-phenylene))bis(oxy))dianiline, but isolating the analogous chalky solid for each of these two was not successful.

Polyimidization:

Once the diamine had been adequately purified, efforts turned to polymerization. The BTDA used in polymerization had to be recrystallized before use, as out of the bottle it is only 96% pure.

In order to ascertain the optimal procedure for polymerization, three different experiments were carried out exploring the TED/BTDA poly(amic acid) production. The first was carried out by first dissolving TED and BTDA in separate fractions of N-methyl-2-pyrrolidinone and adding the solution of BTDA dropwise to the TED solution at 0°C; the second followed the exact same procedure, but at room temperature. In the third, TED was dissolved in NMP and the BTDA was added as a solid in small amounts. The remaining NMP was then added to the mixture. In all three cases, the mixture was allowed to react overnight with stirring.

The third procedure in which the BTDA was added as a solid was found to produce the most viscous poly(amic acid) solution and was the only solution out of the three to produce a creaseable film. The procedure in which the BTDA was added as a solution at room temperature was found to result in the worst polymer of the three.

In carrying out the same procedure with TMD and TBD in place of TED, several polymer films were produced, all of which were uncreaseable. This may have been due to incomplete drying of the diamines. It has also been suggested that if the polymer backbone is sufficiently rigid, the polymer may be uncreaseable even at high molecular weights.

Thermogravimetric analysis (TGA) data along with glass transition temperatures for the three polymers are shown below in Table (1).

Gadolinium Addition:

Production and addition of the gadolinium phenyl acetate salt proved to be problematic. Despite careful adjustment of stoichiometric ratios and pH, all attempts at producing the gadolinium salt fell short of complete substitution of the phenyl acetate ion for the nitrate ion. All gadolinium salts were sent for elemental analysis. The calculated elemental percentages are as follows: 51.23% C, 3.76% H, 27.95% Gd, and 17.06% O. The attempt which achieved the analysis closest to the desired percentages was low in carbon (49.39%) and high in hydrogen (3.82%). The other attempts were all extremely low in both carbon and hydrogen. It seems likely that there was incomplete substitution of the phenyl acetate on the Gd^{3+} ion. This could potentially cause reduced solubility of the gadolinium salt in NMP relative to the completely substituted salt.

Solubility testing of the most promising sample showed that despite its deviation from the ideal weight percentages, it was soluble in NMP, and so it was decided that experimentation should proceed with addition of the salt to a polymer consisting of TED and BTDA. The TGA was used to evaluate the gadolinium composition of the sample and calculations were carried out to compensate for the deviation from the intended gadolinium salt.

Despite the gadolinium salt's solubility in NMP, it was not soluble in the poly(amic acid) solution, even at a relatively low concentration of 5% gadolinium by weight. Adding the salt to the solution resulted in the formation of large clumps which could only be eliminated through heating and rapid stirring. Upon thermal curing of the poly(amic acid), the gadolinium was visibly unevenly distributed within the resulting

film. The film itself was extremely flakey and could not even be removed from the plate in one piece.

Thermal Properties:

All film samples were subjected to both differential scanning calorimetry (DSC) and thermogravimetric analysis (TGA). In the case of DSC scans, the samples were subjected to a cyclic procedure in which the sample is heated to 300°C, cooled to 60°C and then reheated to 300°C. The TGA data were collected by heating the samples to 600°C at a rate of 10°C/min.

The TGA and DSC data of the TED/BTDA, TMD/BTDA, and TBD/BTDA samples are shown below as well as data for two commercially available polymers for comparison. Polypropylene was chosen as a reference because of its high hydrogen content and poly(4,4'-oxydiphenylene-pyromellitimide) (commercially known as Kapton®) was chosen for its desirable thermal properties.

Sample	Temp (°C) for 5% mass loss	Temp (°C) for 10% mass loss	Temp (°C) for 15% mass loss	Temp (°C) for 20% mass loss	Softening Temp (°C)	Hydrogen Content (mol/g)
TED/BTDA	414	430	441	452	273	0.0504
TMD/BTDA	411	428	438	448	288	0.0551
TBD/BTDA	405	423	436	448	283	0.0565
Polypropylene	390	408	416	421	117	0.1440
Poly(4,4'-oxydiphenylene-pyromellitimide)	539	552	561	569	292	0.0264

Table (1): Polymer thermal properties and hydrogen content.

The data displayed in Table (1) shows the utility of the developed polymers in bridging the gap between the high hydrogen content of aliphatic polymers and the

thermal stability of aromatic polymers. The lowest hydrogen-content polymer out of the three novel polymers still possesses almost twice as much hydrogen than poly(4,4'-oxydiphenylene-pyromellitimide) on a mass/mass basis.

Despite this increase in hydrogen content, the synthesized polymers still display a large increase in thermal stability in comparison to polypropylene. The lowest glass transition temperature of the three occurs in the TED/BTDA polymer. The glass transition temperature of this polymer is still over 100°C higher than the melting point of polypropylene. Even despite low molecular weights in both the TMD/BTDA and TBD/BTDA polymers, these polymers still possess higher thermal degradation points and softening temperatures than polypropylene.

The moderate thermal properties of the synthesized polymers are consistent with their overall structures as compared to those of polypropylene or poly(4,4'-oxydiphenylene-pyromellitimide). The polymers undergo 5% thermal degradation between 405°C and 415°C, which is lower than that of poly(4,4'-oxydiphenylene-pyromellitimide), but higher than that of polypropylene owing to aliphatic linkages' increased susceptibility to thermal degradation.

The glass transition temperatures of the polymers also, unsurprisingly, lie between those of poly(4,4'-oxydiphenylene-pyromellitimide) and polypropylene. This is a result of the increased rigidity of aromatic groups which restrict rotation about the carbon-carbon bond to a greater extent than acyclic aliphatic groups, as does the cyclohexylene unit present in each of the synthesized polymers.

Figure (15) illustrates the molecular structures of a number of polyimides which have been produced in this lab by other researchers, along with the polymers' glass transition temperatures.

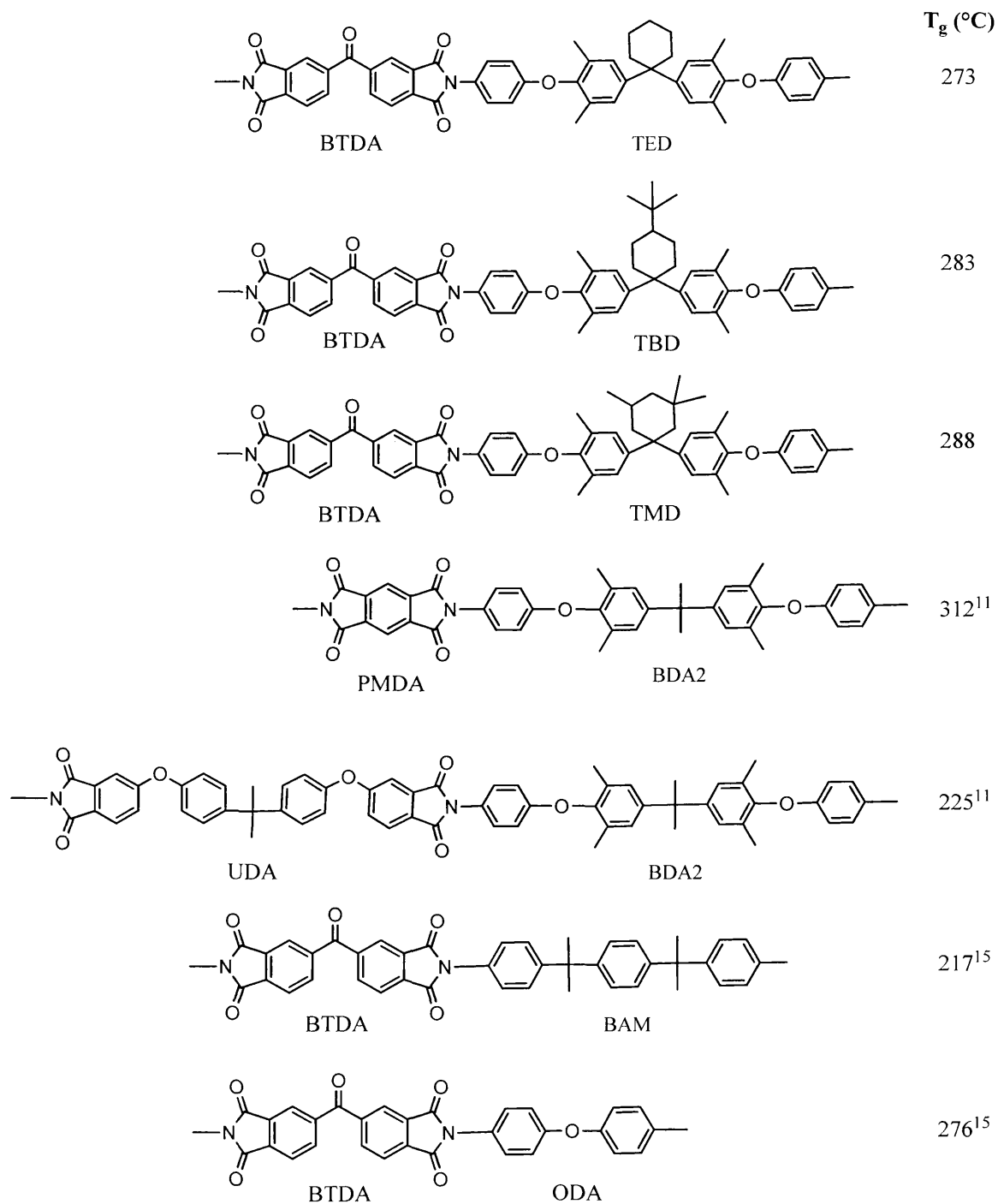


Figure (15): Polyimides and their glass transition temperatures.

The polymers described in this paper have the highest glass transition temperatures of those listed in Figure (15) save one. The increased aromatic character of the BDA2/PMDA polymer and its rigid PMDA unit are likely responsible for the increased T_g .

The glass transition temperature of a polymer is the borderline over which the polymer changes from a brittle, unyielding state to a flexible material. Below the T_g , the polymer molecules are locked in place, unable to move. Above the T_g , the polymer chains are able to flex and move. The more rigid the polymer backbone is on a molecular level, the greater the thermal energy required to obtain this transition.

The rigidity of the backbone is a function of many variables, among them the bulkiness of the polymer chains, the torsional flexibility of the backbone, and the “kinkiness” of the polymer backbone.

Increased bulkiness requires increased space between two adjacent polymer chains before the chains can move freely. Increasing amounts of thermal energy are required as the space needed for flexibility is increased. Thus, bulkier polymers are likely to have high T_g s compared to their less bulky counterparts. This is illustrated in the increase in T_g from TED/BTDA to TMD/BTDA to TBD/BTDA. The bulkier cyclohexylene units of the TMD and TBD polymers in comparison to the TED polymer mean that the TMD and TBD polymers require larger thermal expansion before they become flexible.

Both the torsional flexibility and “kinkiness” of the polymer chain affect the backbone’s ability to move about. The single bond connecting a phenyl carbon to the middle carbon of the isopropylidene unit of Bisphenol-A allows for a large degree of

rotation, allowing for increased backbone flexibility. TED, TMD, and TBD all contain a cyclohexylene unit, which is more hindered, in place of the isopropylidene. This restricts rotational flexibility. The flexibility of those polymers with the isopropylidene units allows for lower glass transition temperatures in comparison to those without.

The relatively high glass transition temperatures of the above polymers containing BTDA can be attributed, in part, to the increased energy required for rotation at the carbonyl carbon. The partial double bond character existing in the bond between the carbonyl carbon and the phenyl ring allows for conjugation which increases the rigidity of the bond, making the molecule less flexible and increasing the T_g . The polymer containing PMDA has a higher T_g than any of the BTDA-containing polymers, owing to its fused ring system, which is extremely rigid.

The hydrogen content of these polymers is shown below as Table (2).

Polymer	Hydrogen Content (mol/g)
TED/BTDA	0.0504
TBD/BTDA	0.0551
TMD/BTDA	0.0565
BDA2/PMDA	0.0493
BDA2/UDA	0.0526
BAM/BTDA	0.0476
ODA/BTDA	0.0288

Table (2): Hydrogen content of selected polyimides.

In addition to their good thermal qualities, the three polymers synthesized in the course of this research have high hydrogen content relative to the others shown in Figure (15). The TBD/BTDA and TMD/BTDA polymers have the highest hydrogen content while the TED/BTDA falls fourth in line for overall hydrogen content, just behind the BDA2/UDA polymer.

CONCLUSION:

Current radiation shielding materials are insufficient for use in deep space exploration. Before long-term missions can be undertaken, it is necessary to produce materials which provide adequate protection for both astronauts and equipment.

In the course of this research, high hydrogen-content aromatic polymers have been explored for their utility in regards to both radiation shielding and as possible structural components. Specifically, polyimides have been explored because of their potential for high thermal stability, dimensional stability, and compressive strength, as well as their resistance to acids, solvents, alkalis, and flames.

Previous research¹³ has been continued to produce three new compounds—5,5'-(3,3,5-trimethylcyclohexane-1,1-diyl)bis(1,3-dimethyl-2-(4-nitrophenoxy)benzene), 4,4'-(((4-(*tert*-butyl)cyclohexane-1,1-diyl)bis(2,6-dimethyl-4,1-phenylene))bis(oxy))dianiline, and 4,4'-(((3,3,5-trimethylcyclohexane-1,1-diyl)bis(2,6-dimethyl-4,1-phenylene))bis(oxy))dianiline. Additionally, polymers have been synthesized by combining each diamine (4,4'-((cyclohexane-1,1-diyl)bis(2,6-dimethyl-4,1-phenylene))bis(oxy))dianiline, 4,4'-(((4-(*tert*-butyl)cyclohexane-1,1-diyl)bis(2,6-dimethyl-4,1-phenylene))bis(oxy))dianiline, and 4,4'-(((3,3,5-trimethylcyclohexane-1,1-diyl)bis(2,6-dimethyl-4,1-phenylene))bis(oxy))dianiline) with BTDA. Out of the three types of polymer, creaseable films were only obtained from the TED/BTDA combination.

The proposed polyimides provide an opportunity for bridging the gap between the thermal stability of high performance aromatic polymers and the high hydrogen content of aliphatic polymers through the presence of the largely aromatic backbone combined

with the high hydrogen-content cyclohexylene unit present in each monomer. Provided creaseable films can be created from the other two diamines, all three polyimides possess adequate thermal stability for use in space applications and improved hydrogen content over traditional aromatic polymers. The main drawback in the overall procedure described in this paper lies in ensuring adequate purity of the diamine. The utmost care must be observed, particularly in purifying the dinitro precursor and in storing the diamine, which oxidizes when exposed to air for any length of time.

FUTURE RESEARCH:

Continuing research should explore the advantages of alternative dianhydrides, which may lend better mechanical qualities to the polymer or increase hydrogen content further. Additionally, neutron and electromagnetic radiation-shielding additives such as boron, tungsten, or other, more efficiently substituted gadolinium salts should be investigated to take the place of the insoluble gadolinium salt explored here. The bisphenol precursors could be utilized in the production of poly(aromatic ethers), which may prove useful in this application. The utility of thick films and the effects of layering should also be examined.

FUNDING:

Funding was provided by International Scientific Technologies, Inc. using a grant from the National Aeronautics and Space Administration.

APPENDIX I

Table 1: Bisphenol crystal and structure refinement data

Figure ID	6a	6b	6c
color and habit	Colorless plates	Colorless blocks	Colorless blocks
size, mm	0.33 x 0.20 x 0.16	0.35 x 0.21 x 0.15	0.24 x 0.17 x 0.07
formula	C ₂₂ H ₂₈ O ₂	C ₂₆ H ₃₆ O ₂	C ₂₅ H ₃₄ O ₂
formula weight	324.44	380.55	366.52
space group	P2(1)/n	P-1	P-1
<i>a</i> , Å	9.51570(10)	9.83030(10)	8.1299(2)
<i>b</i> , Å	19.6052(2)	10.4570(2)	11.0978(3)
<i>c</i> , Å	10.53270(10)	12.1973(3)	12.1268(3)
α , deg	90	98.5750(10)	96.4300(10)
β , deg	114.17	100.3920(10)	91.8410(10)
γ , deg	90	113.4680(10)	109.3940(10)
volume, Å ³	1792.68(3)	1096.80(4)	1022.74(5)
Z	4	2	2
ρ_{calc} , g cm ⁻³	1.202	1.152	1.190
F ₀₀₀	704	416	400
μ (Cu K α), mm ⁻¹	0.581	0.541	0.563
radiation (λ , Å)	CuK α (1.54178)	CuK α (1.54178)	CuK α (1.54178)
temperature, K	100	100	100
residuals: ^a R; R _w	0.0340; 0.0918	0.0375; 0.1016	0.0410; 0.1037
goodness of fit	1.034	1.033	1.018

^aR = $R_I = \Sigma||F_o| - |F_c|| / \Sigma|F_o|$ for observed data only. R_w = $wR_2 = \{\Sigma[w(F_o^2 - F_c^2)^2] / \Sigma[w(F_o^2)^2]\}^{1/2}$ for all data.

Table 2: Dinitro crystal and structure refinement data

Figure ID	7a	7b	7c
color and habit	Yellow-orange plate	Yellow-brown needle	Orange block
size, mm	0.26 x 0.18 x 0.14	0.28 x 0.24 x 0.06	0.32 x 0.28 x 0.12
formula	C34 H34 N2 O6	C38 H42 N2 O6	C39 H44 N2 O8
formula weight	566.63	622.74	668.76
space group	P2(1)/c	P-1	P2(1)/c
a , Å	14.7486(2)	9.8548(2)	12.7021(5)
b , Å	11.18270(10)	10.7153(2)	19.5782(8)
c , Å	34.7669(4)	16.1611(3)	14.1711(6)
α , deg	90	80.8840(10)	90
β , deg	90.3620(10)	72.2820(10)	95.201(2)
γ , deg	90	88.3260(10)	90
volume, Å ³	5733.96(11)	1604.76(5)	3509.6(2)
Z	8	2	4
ρ_{calc} , g cm ⁻³	1.313	1.289	1.266
F_{000}	2400	664	1424
$\mu(\text{Cu K}\alpha)$, mm ⁻¹	0.732	0.700	0.719
radiation (λ , Å)	CuK α (1.54178)	CuK α (1.54178)	CuK α (1.54178)
temperature, K	100	100	100
residuals: ^a R ; R_w	0.0319; 0.0775	0.0384; 0.0991	0.0463; 0.1202
goodness of fit	1.030	1.046	1.041

^a $R = R_I = \sum |F_o| - |F_c| / \sum |F_o|$ for observed data only. $R_w = wR_2 = \{\sum [w(F_o^2 - F_c^2)^2] / \sum [w(F_o^2)^2]\}^{1/2}$ for all data.

Table 3A: Selected bond lengths and angles for 6a

bond lengths (Å)		bond angles (°)	
C(1)-C(15)	1.5409(15)	C(15)-C(1)-C(7)	106.39(8)
C(1)-C(7)	1.5427(15)	C(15)-C(1)-C(6)	111.28(9)
C(1)-C(6)	1.5488(15)	C(7)-C(1)-C(6)	110.53(9)
C(1)-C(2)	1.5536(14)	C(15)-C(1)-C(2)	109.15(8)
		C(7)-C(1)-C(2)	113.03(9)
		C(6)-C(1)-C(2)	106.52(8)

Table 3B: Hydrogen bonds for 6a

D-H...A	d(D-H) [Å]	d(H...A) [Å]	d(D...A) [Å]	<(DHA) [°]
O(1)-H(10)...O(2)#1	0.886(18)	2.126(18)	2.8751(12)	141.8(15)

Table 4A: Selected bond lengths and angles for 6b

bond lengths (Å)		bond angles (°)	
C(1)-C(11)	1.5426(15)	C(11)-C(1)-C(19)	107.03(9)
C(1)-C(19)	1.5438(15)	C(11)-C(1)-C(2)	111.22(9)
C(1)-C(2)	1.5473(15)	C(19)-C(1)-C(2)	110.79(9)
C(1)-C(6)	1.5487(15)	C(11)-C(1)-C(6)	113.02(9)
		C(19)-C(1)-C(6)	108.57(9)
		C(2)-C(1)-C(6)	106.23(9)

Table 4B: Hydrogen bonds for 6b

D-H...A	d(D-H) [Å]	d(H...A) [Å]	d(D...A) [Å]	<(DHA) [°]
O(1)-H(10)...O(2)#1	0.87(2)	2.19(2)	2.9412(12)	143.6(16)

Table 5A: Selected bond lengths and angles for 6c

bond lengths (Å)		bond angles (°)	
C(1)-C(10)	1.5462(16)	C(10)-C(1)-C(18)	106.28(9)
C(1)-C(18)	1.5461(16)	C(10)-C(1)-C(6)	111.17(10)
C(1)-C(6)	1.5472(17)	C(18)-C(1)-C(6)	109.76(10)
C(1)-C(2)	1.5540(17)	C(10)-C(1)-C(2)	113.79(10)
		C(18)-C(1)-C(2)	109.77(10)
		C(6)-C(1)-C(2)	106.07(10)

Table 5B: Hydrogen bonds for 6c

D-H...A	d(D-H) [Å]	d(H...A) [Å]	d(D...A) [Å]	<(DHA) [°]
O(1)-H(10)...O(2)#1	0.88(2)	2.13(2)	2.8974(14)	145.8(18)

Table 6: Selected bond lengths and angles for 7a

bond lengths (Å)		bond angles (°)	
C(1)-C(6)	1.542(2)	C(6)-C(1)-C(21)	111.31(14)
C(1)-C(21)	1.544(2)	C(6)-C(1)-C(7)	111.01(14)
C(1)-C(7)	1.548(2)	C(21)-C(1)-C(7)	108.02(13)
C(1)-C(2)	1.554(2)	C(6)-C(1)-C(2)	106.06(14)
		C(21)-C(1)-C(2)	107.98(14)
		C(7)-C(1)-C(2)	112.47(14)

Table 7: Selected bond lengths and angles for 7b

bond lengths (Å)		bond angles (°)	
C(1)-C(25)	1.5418(19)	C(25)-C(1)-C(6)	110.18(11)
C(1)-C(6)	1.545(2)	C(25)-C(1)-C(11)	106.69(11)
C(1)-C(11)	1.5468(19)	C(6)-C(1)-C(11)	112.60(11)
C(1)-C(2)	1.556(2)	C(25)-C(1)-C(2)	109.63(11)
		C(6)-C(1)-C(2)	105.57(11)
		C(11)-C(1)-C(2)	112.20(12)

Table 8: Selected bond lengths and angles for 7c

bond lengths (Å)		bond angles (°)	
C(1)-C(10)	1.5425(19)	C(10)-C(1)-C(24)	106.42(11)
C(1)-C(24)	1.5440(19)	C(10)-C(1)-C(6)	111.67(11)
C(1)-C(6)	1.5495(19)	C(24)-C(1)-C(6)	110.78(11)
C(1)-C(2)	1.5535(19)	C(10)-C(1)-C(2)	112.84(11)
		C(24)-C(1)-C(2)	108.65(11)
		C(6)-C(1)-C(2)	106.49(11)

REFERENCES

- ¹ Churchill, R; Aquino, E; Orwoll, R; Kiefer R; “Multifunctional Polymers Incorporating High-Z Neutron-Capture Nanoparticles,” NASA Phase I Proposal, 2006.
- ² DuPont™. “Summary of Properties for Kapton® Polyimide Films,” December 28, 2010. <http://www2.dupont.com/Kapton/en_US/assets/downloads/pdf/summaryofprop.pdf>.
- ³ Harper, Charles A.; *Modern Plastics Handbook*; McGraw-Hill Professional Publishing. 2000.
- ⁴ Sroog, Cyrus E. Polyimides (Introduction and Overview). In *Polymeric Materials Encyclopedia*; Salamone, Joseph C., Ed.; CRC Press: New York, 1996; Vol. 128; Pp. 6249-6261.
- ⁵ Rabilloud, Guy. *High Performance Polymers, Vol. 2*; Institut Français du Pétrole Publications: Paris, 1999.
- ⁶ Churchill, R; Aquino, E; Orwoll, R; Kiefer R; “Hydrogen-Rich, Multifunctional Polymeric Nanocomposites for Radiation Shielding,” NASA Phase I Proposal, 2007.
- ⁷ Weber, Edwin; Helbig, Cornelia; Seichter, Wilhelm; Czugler, Matyas. A New Functional Cyclophane Host. Synthesis, Complex Formation and Crystal Structures of Three Inclusion Compounds. *Journal of Inclusion Phenomena and Macrocyclic Chemistry*, **43**(3-4), 239-246 (2002).
- ⁸ Schnell, H.; Krimm, H. Formation and Cleavage of Dihydroxydiarylmethane Derivatives. *Angew. Chem.*, **75**(14), 662-668 (1963).
- ⁹ McGreal, Martin E.; Niederl, Victor; Niederl, Joseph B. Condensation of Ketones with Phenols. *Journal of the American Chemical Society*, **61**, 345-348 (1939).
- ¹⁰ *CRC Handbook of Chemistry and Physics, 82nd ed.*; Lide, David, Ed.; CRC Press: New York, 2001.
- ¹¹ Hu, L.Y, S. Yang, A.K. Miller, C.S. Park, K.A. Plichta, S.J. Rochford, M.E. Schulz, R.A. Orwoll, and B.J. Jensen, Aliphatic/Aromatic Hybrid Polymers for Functionally Graded Radiation Shielding, *High Performance Polymers*, **18**, 213-25 (2006).
- ¹² Personal communication with Dr. Christopher Abelt, College of William and Mary.
- ¹³ Bate, Norah G; “Monomer and Polyimide Production for Radiation Shielding Purposes in Manned Space Exploration.” College of William and Mary, 2009.
- ¹⁴ Personal communication with Dr. Robert Hinkle, College of William and Mary.
- ¹⁵ Harbert, Emily; “Multifunctional Polymer Synthesis and Incorporation of Gadolinium Compounds and Modified Tungsten Nanoparticles for Improvement of Radiation Shielding for Use in Outer Space.” Masters Dissertation, College of William and Mary, 2010.